Article

Transpiration and Water Use of an Irrigated Traditional Olive Grove with Sap-Flow Observations and the FAO56 Dual Crop Coefficient Approach

Àngela Puig-Sirera [1], Giovanni Rallo [2,*], Paula Paredes [3], Teresa A. Paço [3], Mario Minacapilli [4], Giuseppe Provenzano [4] and Luis S. Pereira [3]

[1] Institute for Mediterranean Agricultural and Forestry Systems, National Research Council, P. le Enrico Fermi 1, 80055 Portici, Italy; angeverd8@gmail.com

[2] Laboratory of AgroHydrological Sensing and Modeling (AgrHySMo), Dipartimento di Scienze Agrarie, Alimentari e Agro-ambientali, Università di Pisa, Via del Borghetto 80, 56124 Pisa, Italy

[3] Centro de Investigação em Agronomia, Alimentos, Ambiente e Paisagem (LEAF), Instituto Superior de Agronomia, Universidade de Lisboa, Tapada da Ajuda, 1349-017 Lisboa, Portugal; pparedes@isa.ulisboa.pt (P.P.); tapaco@isa.ulisboa.pt (T.A.P.); luis.santospereira@gmail.com (L.S.P.)

[4] Department of Agricultural, Food and Forest Sciences (SAAF), Università degli Studi di Palermo, Viale delle Scienze, 12, 90128 Palermo, Italy; mario.minacapilli@unipa.it (M.M.); giuseppe.provenzano@unipa.it (G.P.)

* Correspondence: giovanni.rallo@unipi.it

Abstract: The SIMDualKc model was applied to evaluate the crop water use and the crop coefficient (K_c) of an irrigated olive grove (*Olea europaea* L.) located in Sicily, Italy, using experimental data collected from two crop seasons. The model applies the FAO56 dual K_c approach to compute the actual crop evapotranspiration ($ET_{c\,act}$) and its components, i.e., the actual tree transpiration ($T_{c\,act}$), obtained through the basal crop coefficient (K_{cb}), and soil evaporation according to an evaporation coefficient (K_e). Model calibration was performed by minimizing the difference between the predicted $T_{c\,act}$ and the observed daily tree transpiration measured with sap flow instrumentation ($T_{SF\,field}$) acquired in 2009. The validation was performed using the independent data set of sap flow measurements from 2011. The calibrated K_{cb} was equal to 0.30 for the initial and non-growing season stages, 0.42 for the mid-season, and 0.37 for the end season. For both seasons, the goodness-of-fit indicators relative to comparing $T_{SF\,field}$ with the simulated $T_{c\,act}$ resulted in root mean square errors (RMSE) lower than 0.27 mm d^{-1} and a slope of the linear regression close to 1.0 ($0.94 \leq b_0 \leq 1.00$). The olive grove water balance simulated with SIMDualKc produced a ratio between soil evaporation (E_s) and $ET_{c\,act}$ that averaged 39%. The ratio between actual ($ET_{c\,act}$) and potential crop evapotranspiration (ET_c) varied from 84% to about 99% in the mid-season, indicating that the values of $ET_{c\,act}$ are close to ET_c, i.e., the adopted deficit irrigation led to limited water stress. The results confirm the suitability of the SIMDualKc model to apply the FAO56 dual K_c approach to tree crops, thus assessing the water use of olives and supporting the development of appropriate irrigation management tools that are usable by farmers. A different way to estimate K_{cb} is based on the approach suggested in 2009 by Allen and Pereira (A&P), which involves the measured fraction of ground covered (shaded) by the crop and the height of the trees. Its application to the studied grove produced the mid-season K_{cb} values ranging from 0.40–0.45 and end-season K_{cb} values ranging from 0.35–0.40. The comparison between the A&P-computed $T_{c\,act\,A\&P}$ and $T_{SF\,field}$ shows RMSE values ranging from 0.27 to 0.43 mm d^{-1}, which demonstrates the adequacy of the latter approach for parameterizing water balance models and for irrigation scheduling decision making.

Keywords: standard basal crop coefficient; actual transpiration; soil evaporation; sap flow; orchard water balance; fraction of ground cover; K_{cb} from cover fraction and height

1. Introduction

Olives (*Olea europaea* L.) represent one of the most important perennial crops in the Mediterranean agricultural system, in terms of both the quantities produced and the extent of the cultivated area. Italy ranks second in the world, after Spain, with the main producing areas located in Southern Italy. Olives have been cultivated since ancient times in the Mediterranean basin. Traditional olive groves are frequently grown in terraces, and are rain-fed, with low planting densities and a low degree of mechanization. At present, those olive groves have questionable sustainability [1,2]. Therefore, many olive groves have been transformed into irrigated intensive or super-intensive orchard systems, of which the cropped areas continue to increase [3–5]. New olive-production systems consist of very high-density drip-irrigated orchards, with up to 2000 trees/ha, which are well adapted for full mechanization [6,7]. These production systems provide high economic returns but are quite demanding in terms of water, capital and management [8]. Their demand for water faces increased competition with other agricultural and non-agricultural water users, and climate change adds to the uncertainty associated with the quantity and distribution of rainfall throughout the crop season, affecting the sustainability of olive groves [2]. Consequently, the accurate prediction of water use throughout crop seasons, i.e., crop evapotranspiration (ET_c), is essential for accurate irrigation management and for the adoption of water-saving measures [9–11].

The potential ET_c for olive groves is commonly estimated using the FAO56 K_c-ET_o approach, which combines the grass reference evapotranspiration value, ET_o, defining the atmospheric evaporative demand, and a crop coefficient, K_c, reproducing the differences between the bio-physical characteristics of the grass reference crop (canopy properties, ground cover, aerodynamic resistance) and the studied crop [12,13]. The FAO56 K_c-ET_o approach can be applied with a single or a dual crop coefficient. In the former, soil evaporation and crop transpiration are merged into a single K_c value for each crop stage; in the latter, the daily plant transpiration is based on the basal crop coefficient (K_{cb}), whereas the daily soil evaporation is estimated using an evaporation coefficient (K_e). Thus, ET_c is split into crop transpiration ($T_c = K_{cb} ET_o$) and soil evaporation ($E_s = K_e ET_o$). The standard tabulated K_c and K_{cb} values for trees and vines were recently reviewed and updated [14].

The standard tabulated values of K_c and K_{cb} allow ET_c to be evaluated under potential and well-watered conditions [12]. However, under natural field conditions, the crop is often subjected to biotic and abiotic stress due to water deficits caused by insufficient irrigation, inappropriate management practices, soil quality and salinity, or unsuitable crop varieties. Thus, a water stress coefficient, K_s, ranging between 0 and 1.0, is introduced as a multiplicative factor to estimate actual values of K_c or K_{cb}, i.e., $K_{c\ act}$ or $K_{cb\ act}$. The actual crop evapotranspiration ($ET_{c\ act}$) is generally smaller than the potential value (ET_c) and can be defined as

$$ET_{c\ act} = (K_s K_{cb} + K_e) ET_o = K_{c\ act} ET_o \tag{1}$$

Olive crop water requirements, in addition to climate, cultivar and orchard management, depend on crop training, which influences crop height and the fraction of ground cover that results from the tree size and density, as well as on the frequency of irrigation and rain events, which affect the wetted fraction of the soil surface [5,15]. Moreover, woody perennial crops such as olives are characterized by sparse vegetation, with a large fraction of the soil not covered and directly exposed to solar irradiance, and thus subjected to soil evaporation (E_s). The latter, therefore, represents an important fraction of crop ET. For sparse vegetation systems, the dual crop coefficient approach has to be considered more accurate than the single K_c because it allows for the separate estimation of T_c and E_s, thus accounting for the effects of wetting events and soil management practices on the different terms of the water balance [5]. A wide review on crop coefficients for trees and vines [14] has shown that the variability in K_c values is large and much greater than the variability in K_{cb} values, particularly by the end season, as well as in the initial and the late seasons, which results from rainfall events occurring during these periods. Aiming at ET partitioning [16], studies have been carried out based on soil evaporation, measured in mi-

crolysimeters; actual crop transpiration, determined with sap flow sensors [5,17,18]; and/or actual crop evapotranspiration, obtained using eddy covariance techniques [4,19,20], as reviewed by Pereira et al. [21]. A different approach that is currently used is remote sensing, namely, exploring the relationships between $K_{cb\ act}$ and a spectral vegetation index [22–25], which allows its use, together with ground data, in modeling [21]. Properly calibrated models may be used to evaluate crop water requirements, to support proper irrigation management and to evaluate the impact of crops and management, even under the application of water deficit strategies. However, models implement different structures and often do not apply the FAO K_c-ET_o approach, e.g., in the remote sensing-based two-source energy balance algorithm [19] and the transient model Hydrus-2D [26]. Further examples were recently reviewed [21]. Among the dual K_c models, the SIMDualKc model [27,28] is used in the present study since it applies the FAO dual-K_c approach, which is suitable for olive orchards [4,5] and other woody perennial crops, such as vineyards [29,30] and peach trees [7].

As an alternative to the use of models, Allen and Pereira [31] proposed the A&P approach for estimating K_{cb} and/or K_c, adopting a density coefficient (K_d), which is calculated based on observations of the fraction of the ground covered (shaded) by the plants' canopy (f_c) and the crop height (h). The estimation also takes into consideration two other parameters, the multiplier on f_c describing the effect of canopy density (M_L) and the resistance correction factor (F_r). M_L represents the canopy's transparency to solar radiation while F_r is an empirical downward adjustment when the vegetation exhibits more stomatal adjustment on transpiration. The value of f_c may be measured using ground or remotely sensed data [32]. Application examples are provided in other publications [5,25]. A full review of parameter values for M_L and F_r allowed the calibration of these parameters for numerous annual and perennial crops, including olives [33]. The resulting tabulated F_r and M_L parameters are therefore available for the application of the A&P approach, but require validation, which is provided in the current study.

The objectives of this article consist of determining and analyzing the seasonal dynamics of the K_c and K_{cb} values of the studied traditional olive grove and partitioning $ET_{c\ act}$ into actual crop transpiration and soil evaporation, thus assessing the terms of the water balance. These objectives are innovative in terms of the calibration and validation of the SIMDualKc model in a traditional olive grove using measured sap-flow and meteorological data, aiming to use the model to support the irrigation water management of olive groves. Our objectives also include the testing of the recently parameterized A&P approach to derive K_{cb} from the observed f_c and h values and the tabulated M_L and F_r [33], which can be considered a useful approach to improving irrigation management in the field practice.

2. Materials and Methods

2.1. Site Description and Crop Characterization

The field data acquisition was carried out during 2009 and 2011 in the olive field of "Tenute Rocchetta", located in Castelvetrano, Sicily (37°64′94″ N, 12°84′92″ E, 123 m a.s.l.). Climatic and irrigation data and crop characteristics were also available for 2010 and could be used for simulations but not for model assessments. The olive grove (*Olea europaea L.*, var. *Nocellara del Belice*) covers 13 ha, with a plant density of 250 trees/ha spaced 5.0 m along the row, which are roughly oriented from East to West, with 8.0 m between rows [26]. Rallo et al. [18] previously described the studied orchard and reported an average crop height of about 3.5 m and an average effective root depth of 1.0 m. The soil textural class, down to a depth of 1.0 m, is sandy clay loam (clay = 24%, silt = 16%, and sand = 60%). The average soil water content at the field capacity at the same depth is equal to 0.32 cm^3 cm^{-3}, whereas the soil water content at the wilting point is equal to 0.08 cm^3 cm^{-3}. At a 1.0 m depth, the total available water (TAW) equals 240 mm. The total (TEW) and readily (REW) evaporable water were initially estimated according to Allen et al. [12,16] and then modified during the model calibration. More details on the physical characterization of the soil profile are provided in [34,35]. The climate is the typical Mediterranean, with

annual rainfall ranging between 600 and 800 mm, most of which is concentrated in fall and winter; the average monthly temperatures range from 9 °C to 24 °C respectively in January and July.

The agrometeorological data were available from a weather station with standard equipment installed by the Servizio Informativo Agrometeorologico Siciliano (SIAS), located northwest of the experimental site, at a distance of about 500 m. Moreover, a four-component net radiometer (NR01, Hukseflux, Manorville, New York, NY, USA), installed above the crop canopy at 5.60 m from the ground, allowed the monitoring of the net radiation (R_n) and its components. The weather station provided hourly measurements of standard climate variables (incoming short-wave solar radiation, air temperature and air humidity at 2 m height, wind velocity and direction at 10 m height, and daily precipitation). The monitored climate variables were used to estimate the reference crop evapotranspiration (ET_o, mm d^{-1}) using the PM-ET_o equation [12]. Figure 1 shows the main daily climate variables observed in the period 2009–2011.
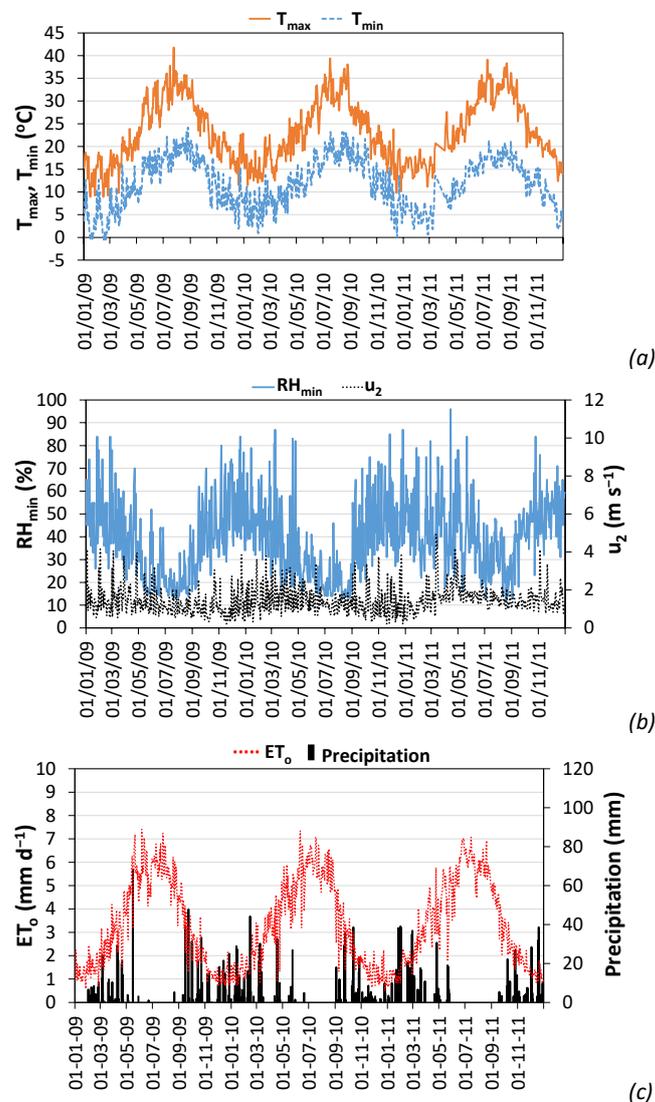

Figure 1. Main daily-observed climatic variables at the weather station of Castelvetrano in 2009, 2010, and 2011: (**a**) maximum (T_{max}) and minimum (T_{min}) temperatures, (**b**) minimum relative air humidity (RH_{min}) and wind speed at 2 m height (u_2), and (**c**) precipitation and FAO Penman–Monteith reference crop evapotranspiration (ET_o).

The dates defining the beginning and the end of crop phenological stages are indicated in Table 1 for the three years of study. They follow the FAO56 guidelines [12] adapted to evergreen trees, thus including a non-growing stage, which corresponds to the period of dormancy of the crop. The initial stage starts when the dormancy ends at budburst after chilling requirements are completed and the cumulative degree-days satisfy the heat requirements. The dates from the beginning of the initiation until the late season (Table 1) are analogous to those considered by other authors [36–39]. The initiation stage is rather short, and the crop development stage runs until the initiation of flowering. The mid-season is the longest stage and ends at the beginning of fruit maturity.

Table 1. Dates of the beginning and end of the crop growth stages.

	Crop Growth Stages					
Season	**Non-Growing**	**Initial**	**Crop Development**	**Mid-Season**	**Late Season**	**Non-Growing**
2009	01/01–09/03	10/03–24/03	25/03–07/05	08/05–30/09	01/10–15/11	16/11–31/12
2010	01/01–08/03	09/03–28/03	29/03–14/05	15/05–29/09	30/09–22/11	23/11–31/12
2011	01/01–07/03	08/03–20/03	21/03–30/04	1/05–11/10	12/10–17/11	18/11–31/12

Irrigation water was applied using a drip irrigation system with drip-lines placed along the crop rows with four 1.0 m-spaced on-line auto-compensating emitters per tree, having a nominal discharge of 8 L h^{-1}. After irrigation, the soil wetted fraction f_w was observed to average 0.11 [18]. Observations of f_w [12] were determined by simply measuring the ground surface wetted by a few emitters. The fraction of ground covered (shaded) by vegetation (f_c) was visually estimated using photographs of the ground shadow taken 2 m above the tree canopy near solar noon and was estimated to be approximately 0.35 during the mid-season and the end season [18,40]. Seasonal irrigation depths, supplied according to the farmer's decision, were 81, 33, and 150 mm respectively for 2009, 2010, and 2011. Table 2 summarizes the amounts of precipitation and irrigation applied to the field at each crop stage during those three years.

Table 2. Precipitation (mm) and net irrigation depths (mm) in each crop growth stage of the three years.

Crop Growth Stages	2009		2010		2011	
	Precipitation (mm)	**Irrigation (mm)**	**Precipitation (mm)**	**Irrigation (mm)**	**Precipitation (mm)**	**Irrigation (mm)**
Non-growing *	239	0	323	0	711	0
Initial	26	0	60	0	63	0
Development	128	0	51	0	101	0
Mid-season	210	81	157	33	77	150
Late-season	154	0	145	0	187	0
Total	757	81	736	33	1139	150

* includes the two non-growing seasons as defined in Table 1.

2.2. Sap Flow and Transpiration Data

The hourly transpiration of three olive trees having trunk diameter dimensions representative of the whole field was estimated based on sap-flow measurements and the heat dissipation technique (HDT) [41], from day of the year (DOY) 160 to 276 in 2009, and 130 to 306 in 2011 [18]. HDT involves direct measurements in the trunk section. It consists of two short needles inserted radially into the trunk at a distance of about 10 cm and equipped with two thermocouples, allowing one to measure the difference in temperature (ΔT) between them. Therefore, HDT measures the heat dissipated in the sapwood, which rises with increasing sap flow. The lower the sap-flow velocity, the higher the temperature difference between the two needles due to the reduced dissipation of heat from the heated

upper needle. Hence, on a daily time step, the maximum difference in temperature between the probes (ΔT_{max}) indicates minimum or null flux in the sapwood [41–43].

The sap flow density ν (m^3 m^{-2} s^{-1}), is calculated with a species-independent relationship, calibrated empirically [44]:

$$\nu = 0.714 \left(\frac{\Delta T_{max} - \Delta T}{\Delta T} \right)^{1.231} \tag{2}$$

where ΔT is the difference in temperature and ΔT_{max} is the maximum value of ΔT. The knowledge of the conductive xylem area, A (m^2), allows the calculation of the sap flux F (m^3 s^{-1}) as:

$$F = \nu A \tag{3}$$

This method has been used in several studies, including with olive trees [4,23,43]. In each monitored olive tree, two thermal dissipation probes (TDPs) (SFS2 TypM-M, UP GmbH Firmensitz, Ibbenbüren, Germany) were installed in the concave and convex part of the trunk exposed to the north side, at about 40 cm from the ground, and insulated to avoid direct sun exposure. All the probes were connected to a CR1000 datalogger (Campbell Scientific Inc., Logan, Utah) and acquired at an hourly time step.

The sapwood area was determined at the end of the experiment by measuring the sapwood depths of six cores extracted with a Pressler gimlet [18].

For each tree, the daily integral of hourly sap fluxes, F, computed with Equation (3) was assumed as corresponding to tree transpiration, after neglecting the effects of tree capacitance [45], at a daily time step. The daily transpiration depth ($T_{SF\ plant}$, mm d^{-1}) was determined as the ratio between the daily flux (l d^{-1}) and the area dominated by a single tree, A_{plant} = 40 m^2. Then, to upscale $T_{SF\ plant}$ to the whole field ($T_{SF\ field}$), the average leaf area index measured in the field (LAI_{field}, m^2 m^{-2}) was normalized according to the corresponding LAI obtained for the same tree where sap flow sensors were installed (LAI_{plant}, m^2 m^{-2}); thus, it was assumed as the proximal variable:

$$T_{SF\ field} = T_{SF\ plant} \frac{LAI_{field}}{LAI_{plant}} \tag{4}$$

The values of LAI_{field} and LAI_{plant} were measured with the LAI-2000 (Li-Cor Inc., Lincoln, NE, USA) as proposed by Villalobos et al. [46] and explained in detail by Cammalleri et al. [23]. The average LAI_{field} and LAI_{plant} were 0.89 and 1.27, respectively [18,23].

2.3. The SIMDualKc Model and Simulation of Transpiration Fluxes

The SIMDualKc soil water balance model [27,28] adopts the dual crop coefficient approach proposed in FAO56 [12,16] to compute both components of $ET_{c\ act}$ with a daily time step. The resulting model outputs of actual transpiration ($T_{c\ act}$, mm) and soil evaporation (E_s, mm) fluxes are suitable to assess the fate of the water used by the crop (precipitation and irrigation), which is of particular interest for partial-cover woody perennial crops, as demonstrated in previous model applications [4,5,7,29].

The model algorithms are detailed by Rosa et al. [27] and were recently described by Pereira et al. [21]. The model presents several options: (a) the computation of crop irrigation water requirements; (b) the calibration and validation of the model for crops cultivated in well-defined environmental and cropping conditions, e.g., with and without ground cover; (c) the development of irrigation scheduling alternatives for field applications; (d) the assessment of a given irrigation schedule; and (e) the computation of water balance terms.

The soil water balance is solved with a daily time step by considering the depletion, D_r, in the root zone at days i and i − 1 as:

$$D_{r,i} = D_{r,i-1} - (P - RO)_i - I_i - CR_i + ET_{c\ act,i} + DP_i \tag{5}$$

where $D_{r,i}$ and $D_{r,i-1}$ (mm) refer to the end of days i and i − 1, respectively; $(P − RO)_i$ is the infiltrated precipitation, obtained as the difference between gross precipitation P_i and runoff RO; I_i, CR_i, $ET_{c\,act,i}$, and DP_i, are respectively the net irrigation, the capillary rise, the actual crop evapotranspiration and the deep percolation, with all terms expressed in mm and referring to the day i. The runoff term is computed according to the curve number method [47], whereas capillary rise and deep percolation are computed according to the method of Liu et al. [48].

Considering Equation (1), the actual daily crop transpiration and soil evaporation are given as:

$$T_{c\,act} = (K_s K_{cb}\,ET_o) = K_{cb\,act}\,ET_o \tag{6}$$

$$E_s = K_e\,ET_o \tag{7}$$

For each day, the stress factor K_s is estimated as a linear function of the root zone depletion D_r (mm):

$$K_s = \frac{TAW - Dr}{TAW - RAW} = \frac{TAW - Dr}{(1-p)\,TAW}\ \text{for}\ D_r > RAW$$

$$K_s = 1\ \text{for}\ D_r \leq RAW \tag{8}$$

where TAW is the total available soil water (mm) and RAW is the readily available soil water (mm), with RAW = p TAW, and p is the soil water depletion fraction for no-stress [12]. $K_s < 1.0$ when the root zone depletion exceeds RAW, i.e., the water depleted fraction is larger than p.

The soil evaporation coefficient, K_e, is maximum immediately after the occurrence of wetting events (rainfall or irrigation) and when the canopy partially covers the wetted soil surface. That maximum depends upon the maximum K_c value ($K_{c\,max}$), which represents the upper limit of evaporation and transpiration from any cropped surface and reflecting the natural constraints placed on available energy upon the transpiration coefficient K_{cb} in the same day, thus upon $K_{c\,max} − K_{cb}$ [12,31,49]. However, it varies daily with the amount of water available for evaporation in the topsoil; K_e is estimated through a dimensionless reduction factor, K_r, as:

$$K_e = K_r\,(K_{c\,max} − K_{cb}) \leq f_{ew}\,K_{c\,max} \tag{9}$$

where f_{ew} represents the fraction of soil wetted and exposed to direct solar radiation, which may be estimated as $f_{ew} = \min(1 − f_c, f_w)$ based on the fractions of ground covered (shaded) by the vegetation canopy (f_c) and wetted by irrigation (f_w). The value of K_r depends upon the cumulative depth of water depleted from the topsoil and is calculated through the daily soil water balance of the soil evaporation layer of thickness Z_e (m). Computations assume that the drying cycle occurs in two stages, the first limited by the available energy at the soil surface and the second by the water available in the topsoil [12,16], thus with K_r decreasing when the evaporated depleted water exceeds the readily evaporable water (REW). Thus, K_r is computed as:

$$K_r = 1\ \text{for}\ D_{e,i-1} \leq RAW$$

$$K_r = \frac{(TEW - D_{e,i-1})}{(TEW - REW)}\ \text{for}\ D_{e,i-1} > REW \tag{10}$$

where $D_{e,i-1}$ is the amount of water evaporated from the evaporable soil layer at the end of day i − 1.

The model input requirements in the current study consider the following data:

(a)　Soil data: soil depth (m); the soil water content at field capacity (θ_{FC}, m^3 m^{-3}) and at the permanent wilting point (θ_{WP}, m^3 m^{-3}), the values of which were measured; the depth of the soil evaporation layer (Z_e, m) and the total and readily evaporable water (TEW and REW, mm), which were estimated based on [12]; and the measured values

of the initial soil water available in the root zone and the Z_e soil layer, expressed as a percentage of TAW and TEW, respectively.

(b) Climatic forcing at the daily time-step: rainfall (P, mm), reference crop evapotranspiration (ET_o, mm d^{-1}), minimum and maximum air temperature (T_{min} and T_{max}, °C), minimum relative air humidity (RH_{min}, %), and wind speed measured at a 2 m height (u_2, m s^{-1}).

(c) Crop data: dates for the start of the crop stages (non-growing, initial, crop development, mid-season, late-season and end-season); initial values of K_{cb} for the considered crop stages; the soil water depletion fraction p for no stress for the same stages; root depth (Z_r, m); tree height (h, m); the fraction of ground covered by vegetation (f_c) at the same stages; and the row orientation and spacing.

(d) Irrigation data: fraction of soil wetted (f_w); applied depths (I_i, mm) and the respective dates.

(e) Other data: the initial default values a_D and b_D for the deep percolation parametric function proposed by Liu et al. [48]; the initial value for the curve number (CN) used to estimate runoff following Allen et al. [47]. Capillary data were not observed because a groundwater table was not present.

Output results refer to the daily variation of soil water availability in the root zone, the actual crop evapotranspiration and transpiration, and of the other terms of the soil water balance related to water use. Intermediate results of computations may also form part of the output data.

2.4. Estimation of K_{cb} Values from Observations of the Fraction of Ground Cover and Crop Height: The A&P Approach

The practical application of the dual K_c approach for supporting field irrigation management may be easier when adopting the A&P approach [31], as recently reviewed in [32,33]. In the A&P approach, $K_{cb\ A\&P}$ is expressed as a function of a density coefficient (K_d). For bare soil in the inter-row, it is estimated as:

$$K_{cb\ A\&P} = K_{c\ min} + K_d(K_{cb\ full} - K_{c\ min}) \tag{11}$$

where $K_{cb\ full}$ is the estimated K_{cb} during peak plant growth for conditions having nearly full ground cover (or LAI > 3), and $K_{c\ min}$ is the minimum basal K_c for bare soil (0.15 under typical agricultural conditions). The density coefficient K_d is estimated from observations of the fraction of the ground covered by vegetation (f_c) and of plant height (h) and describes the increase in K_c with increases in the amount of vegetation. Following [31], K_d is estimated as:

$$K_d = \min\left(1,\ M_L\ f_{c\ eff},\ f_{c\ eff}^{\left(\frac{1}{1+h}\right)}\right) \tag{12}$$

where $f_{c\ eff}$ is the effective fraction of the ground covered or shaded by vegetation (0.01–1) near solar noon, M_L is a multiplier on $f_{c\ eff}$ describing the effect of canopy density on shading and maximum relative ET per fraction of shaded ground (1.0–2.0), and h is the mean vegetation height (m), as recently reviewed [33].

The $K_{cb\ full}$ value in Equation (11) represents an upper limit on $K_{cb\ mid}$ for vegetation under an adequate water supply having a full ground cover and a LAI value higher than 3. Following [12], the $K_{cb\ full}$ value can be approximated as a function of mean h and adjusted for climate conditions as:

$$K_{cb\ full} = F_r\left(\min(1.0 + k_h\ h,\ 1.20) + [0.04(u_2 - 2) - 0.004(RH_{min} - 45)]\left(\frac{h}{3}\right)^{0.3}\right) \tag{13}$$

where u_2 is the average daily wind speed (m s^{-1}) at a height of 2 m above ground level during the growth period, RH_{min} (%) is the average daily minimum relative humidity during the growth period, and h is the mean plant height (m) during the mid-season. Before climatic adjustment, an upper limit for $K_{cb\ full}$ is 1.20 (Equation (13)). The effect of the crop height is considered through the sum ($1 + k_h\ h$), with $k_h = 0.1$ for tree and vine crops [32,33].

Higher $K_{cb\,full}$ (Equation (13)) values are expected for taller crops and in cases in which the local climate is drier or windier than the standard climate conditions (RH_{min} = 45% and u_2 = 2 m s^{-1}). The parameter F_r applies an empirical adjustment ($F_r \leq 1.0$) when the vegetation shows more stomatal adjustment upon transpiration, which is typical of most annual crops. For trees and vines, F_r is high when crops exhibit great vegetative vigor and decreases due to the effect of pruning and training, as well as under a limited water supply. Adopting the definition proposed by Allen et al. [12] for F_r, it is assumed that:

$$F_r = \frac{\Delta + \gamma\,(1 + 0.34\,u_2)}{\Delta + \gamma\left(1 + 0.34\,u_2\frac{r_l}{r_{typ}}\right)} \tag{14}$$

where r_l and r_{typ} are, respectively, the mean leaf resistance and the typical leaf resistance (s m^{-1}) for the vegetation in question, Δ is the slope of the saturation vapor pressure vs. air temperature curve, kPa $^\circ$C^{-1}, and γ is the psychrometric constant, kPa $^\circ$C^{-1}, both relative to the period when $K_{cb\,full}$ is computed. The original version of that equation was established with a fixed r_{typ} = 100 s m^{-1}, a common value for annual crops, but default F_r values were recently reviewed for trees and vines and several annual crops [33].

Examples of the application of the $K_{cb\,A\&P}$ approach to several annual and perennial crops are given by Pereira et al. [32], including for active soil cover in the inter-row. The application of this approach does not require any process of calibration/validation when using the tabulated parameters [33]. However, because data were available, a validation was performed by comparing $K_{cb\,A\&P}$ and K_{cb} computed with the model SIMDualKc.

2.5. SIMDualKc Model Calibration and Validation; Goodness-of-Fit Indicators

The model calibration procedure consisted of progressively adjusting the values of the non-measured parameters, aiming at minimizing the differences between the model-simulated and sap-flow-observed values of daily transpiration, i.e., $T_{c\,act}$ and $T_{SF\,field}$ data, acquired in 2009. The set of adjusted parameters included the K_{cb} and p values relative to each crop growth stage, as well as the parameters used to estimate soil evaporation, deep percolation, and runoff. The initial crop and evaporation parameters were selected from FAO56 and Rallo et al. [18], whereas those relative to DP and RO were obtained from the parameter values proposed by Liu et al. [48] and Allen et al. [47], respectively.

Calibration was performed using a trial-and-error iterative procedure to minimize the $T_{c\,act}$ estimation errors [50]. The trial-and-error procedure consisted, first, of the iterative searching of K_{cb} and p values for the various crop growth stages until the differences in $T_{c\,act} - T_{SF\,field}$ become small and their variations from one iteration to the next were found to be lower than 0.01. After obtaining the best set of K_{cb} and p values, the trial-and-error procedure was applied to CN, and the deep percolation parameters a_D and b_D [48], again aiming at lowering the estimation errors with negligible differences in consecutive iterations. Finally, the procedure was applied again to the crop parameters K_{cb} and p to further reduce the differences in $T_{c\,act} - T_{SF\,field}$.

To evaluate the goodness-of-fit associated with the model simulations during the calibration process, different methodologies were applied. The first referred to the qualitative graphical analysis of the temporal dynamics of simulated and observed $T_{c\,act}$ and $T_{SF\,field}$ values. This analysis allowed us to discern trends or biases in the modeling and therefore to make decisions regarding parameter changes in each iteration. The second step referred to the quantitative evaluation of estimation errors using several goodness-of-fit indicators as in previous studies using SIMDualKc [28,50,51].

Using the calibrated parameters, the model was validated using $T_{SF\,field}$ data acquired in the 2011 season, so the model accuracy was verified by comparing the simulated $T_{c\,act}$ with the observed $T_{SF\,field}$ values in that season. The model accuracy relative to the validation was evaluated with the same goodness-of-fit indicators used at calibration and described below. The calibration/validation process was considered acceptable when the

goodness-of-fit indicators associated with the validation were found to be comparable to those obtained for the calibration [50,52,53].

The goodness-of-fit indicators used to assess the matching of the differences in $T_{c\ act} - T_{SF\ field}$ were as follows:

(a) The regression coefficient (b_0, dimensionless) of the linear regression forced to the origin between the measured and simulated variables; the target value is $b_0 = 1.0$, which indicates that the predicted values are statistically equal to the observed ones;

(b) The coefficient of determination (R^2, dimensionless) of the ordinary least-squares regression between the simulated and observed values; its value should be close to 1.0, indicating that most of the variance of the observed values is explained by the model;

(c) The root mean square error (RMSE, mm d^{-1}), the target value of which is zero, indicating a perfect match between simulated and observed variables, the value of which must be quite smaller than the mean of the observed values;

(d) The average absolute error (AAE, mm d^{-1}), expressing the average error associated with the estimations and which should also be much smaller than the mean of the observed values;

(e) The percent bias (PBIAS, %), measuring the average tendency of the predicted values to be larger or smaller than the corresponding measured pair; positive values correspond to an overestimation bias, whereas negative values indicate under-estimation bias; and

(f) The Nash and Sutcliffe efficiency of modelling (EF, dimensionless) [54], obtained as the ratio between the mean square error (MSE) and the variance of the observed variable (s^2_{obs}), the target value of which, equal to 1.0, indicates that MSE is negligible with respect to s^2_{obs};

Further details and the definition equations relative to the goodness-of-fit indicators are given in various SIMDualKc articles, namely, in [50].

3. Results and Discussion

3.1. Model Calibration and Validation Using Transpiration Measurements

Table 3 summarizes the initial and final values of the parameters considered for the model calibration: K_{cb}, p, TEW, REW, Z_e, CN, a_D, and b_D. The calibrated K_{cb} parameters relative to all crop growth stages were found to be slightly larger than the initial ones and those obtained previously using different modeling approaches [18,23]. The $K_{cb\ non-growing}$ and $K_{cb\ ini}$ values obtained in this study are comparable to those obtained by [5] in a super-intensive hedgerow olive orchard. Moreover, the calibrated K_{cb} values are in the range of those reviewed by [14] and confirm the values proposed by [33].

Table 3. Initial and calibrated parameters used in the SIMDualKc model.

Parameters		Initial Values	Calibrated Values
Crop	$K_{cb\ non-growing}$	0.25	0.30
	$K_{cb\ ini}$	0.25	0.30
	$K_{cb\ mid}$	0.40	0.42
	$K_{cb\ end}$	0.30	0.37
	p_{ini}	0.65	0.65
	p_{dev}	0.65	0.65
	p_{mid}	0.65	0.65
	$p_{maturity}$	0.65	0.65
	p_{end}	0.65	0.65
Soil evaporation	TEW	28	28
	REW	10	10
	Z_e	0.10	0.10
Runoff and deep percolation	CN	72	75
	a_D	320	330
	b_D	−0.0175	−0.0175

The values of the depletion fraction p are equal to those proposed by [12] and similar to those previously adopted in other studies [5,17,18,23]. A value of $p = 0.65$ reflects the tolerance of the olives crop to water stress.

The initial values concerning Z_e, REW, and TEW were estimated according to the soil particle size distribution analysis and the water holding capacity of the evaporation soil layer [12]. Thus, the calibrated soil evaporation parameters are similar to those given in FAO56 for silty-clay-loam soil texture. The calibrated runoff parameter CN slightly changed in respect to the initial value proposed by Allen et al. [47]. The parameters associated with deep percolation consisted of a_D, estimated from the available soil water at saturation and field capacity, and b_D, estimated from the drainage characteristics of the soil [48]. Therefore, their calibrated values are in line with those indicated by these authors for medium-textured soils (Table 3).

Figure 2 compares the simulated and the observed transpiration fluxes during 2009 and 2011. The results for both years show that the temporal variability of both $T_{c\,act}$ and $T_{SF\,field}$ are similar, with the simulated $T_{c\,act}$ matching well the observed $T_{SF\,field}$ when the calibrated parameters were used. Very good indicators of goodness-of-fit were obtained (Table 4).
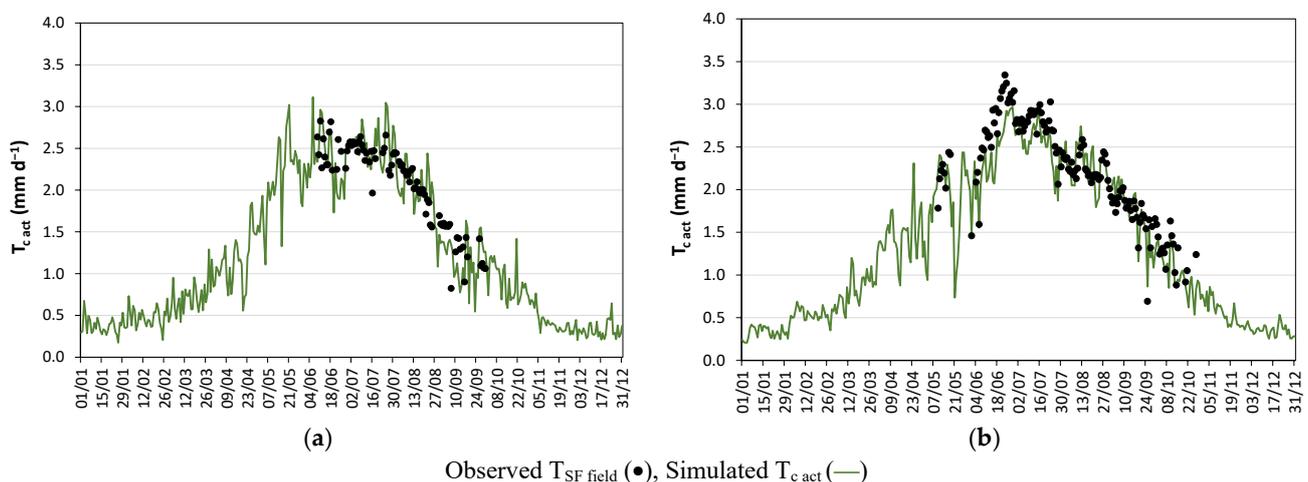

Observed $T_{SF\,field}$ (●), Simulated $T_{c\,act}$ (—)

Figure 2. Actual crop transpiration dynamics measured with sap flow ($T_{SF\,field}$) and simulated with SIMDualKc after model calibration ($T_{c\,act}$) for (**a**) 2009 and (**b**) 2011.

Table 4. Goodness-of-fit indicators relative to the comparison between simulated transpiration ($T_{c\,act}$) and the corresponding values obtained from sap-flow measurements ($T_{SF\,field}$).

	n	b_0	R^2	PBIAS (%)	RMSE (mm d^{-1})	AAE (mm d^{-1})	EF
Calibration, 2009	104	1.00	0.76	0.6	0.27	0.22	0.71
Validation, 2011	145	0.94	0.84	−5.2	0.26	0.20	0.81

b_0—regression coefficient, R^2—coefficient of determination, PBIAS—percent bias, RMSE—root mean square error, AAE—average absolute error, EF—efficiency of modeling.

The regression coefficient b_0 is close to 1.0 in both cases, indicating the statistical similarity of the predicted and observed $T_{c\,act}$ and $T_{SF\,field}$ values. The PBIAS values are consequently small, 0.6% and 5.2%, thus indicating that the simulated $T_{c\,act}$ values do not show large trends for under- or over-estimation bias. The high R^2 values (0.76–0.84) indicate that the model allows us to capture well the temporal variability of crop transpiration.

Estimation errors are small, as indicated by RMSE ≤ 0.27 mm d^{-1} and AAE ≤ 0.22 mm d^{-1}. The EF was high (0.71 and 0.81), implying that the mean square error is much smaller than the measured data variance. Generally, the goodness-of-fit indicators suggest that the model was properly calibrated and performed as a good predictor of transpiration dynamics, and

the calibrated parameters, particularly the basal K_{cb}, may be used with confidence in the field practice.

The goodness-of-fit indicators were of the same magnitude as those estimated in another application comparing the SIMDualKc simulated $T_{c\,act}$ with sap-flow T_{SF} measurements obtained in a super-intensive olive orchard [5]. The $T_{c\,act}$ estimation errors obtained in this study were smaller than those reported by other authors [17,18]. Moreover, it is important to note that the daily variability of transpiration during the study periods was enormous (Figure 3). Similar findings were reported by Villalobos et al. [55].
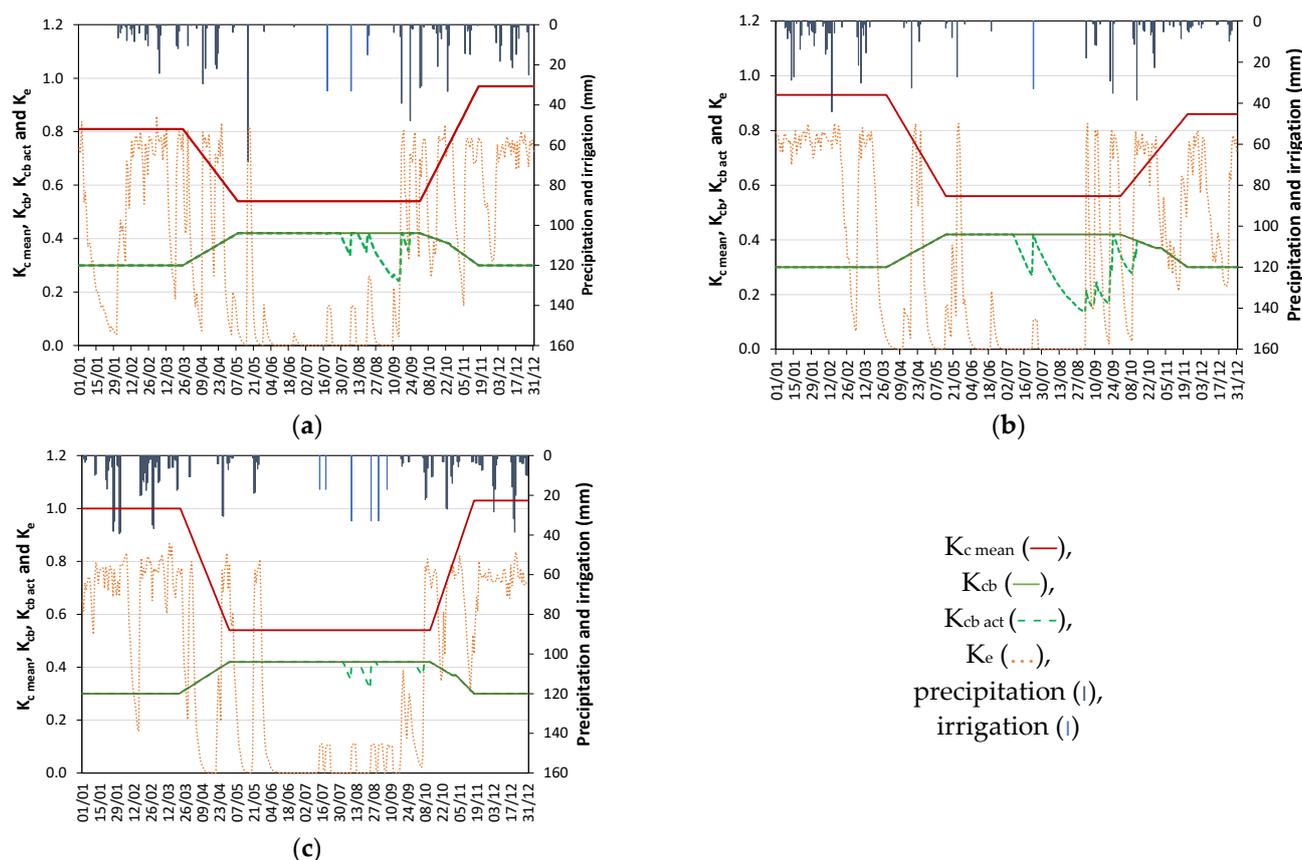

Figure 3. Standard and actual basal crop coefficients (K_{cb}, $K_{cb\,act}$), evaporation coefficient (K_e), and time-averaged standard single crop coefficient ($K_{c\,mean}$) of the olive grove for (**a**) 2009, (**b**) 2010, and (**c**) 2011. Precipitation and irrigation events are also depicted.

3.2. Dynamics of the Single and Basal Crop Coefficients throughout the Season

The K_{cb} and $K_{cb\,act}$ curves, the daily K_e, and the time-averaged single K_c curves estimated using the SIMDualKc model are presented in Figure 3 for the three experimental years. For 2009 and 2011, these curves included sap-flow data, which were not available for 2010. The standard K_c was time-averaged in the different crop stages and calculated as the sum of the daily standard K_{cb} and the corresponding K_e.

The K_{cb} and $K_{cb\,act}$ curves in Figure 3 are coincident ($K_{cb\,act} = K_{cb}$) when rainfall events are sufficient to avoid water stress, i.e., during winter, autumn, and spring. On the contrary, water stress ($K_{cb\,act} < K_{cb}$) occurred for several days during the mid-season of 2009 and 2010 because deficit irrigation was practised, with few irrigation events—three in 2009 and one in 2010 using uncommonly large irrigation depths. By contrast, water stress was not observed in 2011, when six irrigation events were practised. The presented K_c curves reveal a behaviour contrary to the common K_c curves in FAO56, similar to that reported in [5], because soil evaporation was small in summer, when the water use mainly consisted of transpiration.

The soil evaporation curves in Figure 3 show numerous K_e peaks that represent the responses to rainfall and irrigation events during the different stages of crop growth, with peaks in the mid-season mostly corresponding to irrigation events. K_e peaks are larger when responding to rainfall because the ground is entirely wetted ($f_w = 1$). During the mid-season, K_e peaks are small and of short duration; because the wetted and exposed fraction f_{ew} is small, the soil dries out quickly and the ground is shaded by the canopies. Thus, during the mid-season, the reduced soil evaporation is due to the limited energy reaching the soil and the location of the wet areas, which are mostly placed under the shadow of the tree canopy.

The K_c and K_{cb} curves show contradictory dynamics (Figure 3) because K_c values are highly influenced by soil evaporation, whereas K_{cb} values are not. Thus, the time-averaged K_c curve for the mid-season, when E_s is small, is lower than the K_c segments relative to the late and the non-growing seasons, where rainfall occurs, and soil evaporation increases. On the contrary, the standard $K_{cb\,mid}$ values are higher during the mid-season because crop transpiration is high at that time, and K_{cb} is lower outside of this period since transpiration is reduced.

Table 5 presents the time-averaged K_c values for each crop growth stage for the three seasons. The $K_{c\,ini}$ values range from 0.81 to 1.00, following the variability of rainfall in the same period. This range of variation is comparable to that reported in [5] for the $K_{c\,ini}$ values of a super-intensive olive orchard (0.70–0.96). In contrast, other authors obtained smaller $K_{c\,ini}$ values in a hedge-pruned intensive olive orchard, which likely reflects differences in climate [56]. The time-averaged $K_{c\,mid}$ values varied little, from 0.54 to 0.56, for the three study years, resulting in similar values to those reported in [23]. The $K_{c\,mid}$ values are higher than the standard values proposed in [14], which may result from the high number of wetting events in the current study. The $K_{c\,mid}$ values are also larger than those proposed in [33] after using the A&P approach. The $K_{c\,end}$ values are high, ranging from 0.86 to 1.03, due to the occurrence of rainfall events during the late season. These values are in line with those proposed by other authors [5,23,56,57] but are higher than the standard value of $K_{c\,end} = 0.65$ and 0.70, as indicated in [33] and [14], respectively, likely due to the presence of grass on the soil surface and/or the tree age.

Table 5. Time-averaged single crop coefficients (K_c) for each crop growth stage.

Crop Growth Stages	2009	2010	2011	Average
Non-growing *	0.87	0.90	1.01	0.93
Initial	0.81	0.93	1.00	0.92
Mid-season	0.54	0.56	0.54	0.55
End season	0.97	0.86	1.03	0.95

* average value relative to both non-growing periods, by the end and the beginning of the year.

3.3. Soil Water Balance and Water Use

The different values of the soil water balance, computed with SIMDualKc for the three years, are summarized in Figure 4. The observed differences among years are due to the inter-annual variability of precipitation, and its distribution during the various crop growth stages.
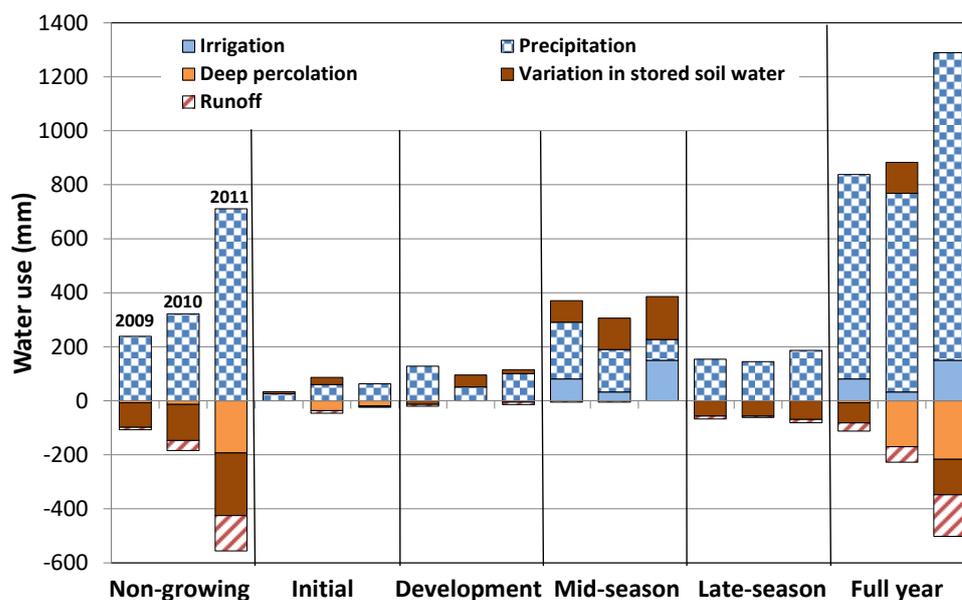
Figure 4. Simulated soil water balance components (all variables in mm) after proper model calibration for the three studied years 2009–2011.

The wettest year was 2011, with higher runoff and deep percolation (RO and DP, mm) than in the other two years. In 2011, RO and DP represented 33% of precipitation, which can be contrasted with the low values observed in 2009, when they corresponded to only 5% of precipitation. In 2010, RO and DP corresponded to about 31% of the precipitation. In the wet year of 2011, runoff represented the smallest fraction of precipitation (14%), less than DP (19%). These percentages indicate that in 2011 the rainfall was mostly used as crop evapotranspiration. The largest amounts of RO and DP mainly occurred during the rainy season, corresponding to the non-growing crop stage, in a period with the smallest crop ET (Table 6). RO and DP did not originate from excess irrigation, which would occur during the mid-season when both the variables were nearly null.

Irrigation events occurred only during the mid-season and corresponded to 22%, 11% and 39% of $ET_{c\,act}$ in 2009, 2010, and 2011, respectively (Table 2). Irrigation events were more frequent in 2011, resulting in smaller variations in the stored soil water and fewer days with crop water stress compared to the other years. Consequently, in 2011, with higher precipitation and more adequate irrigation, both $T_{c\,act}$ and $ET_{c\,act}$ were larger (Table 6). Because of irrigation events, the contribution of soil water storage to $ET_{c\,act}$ is larger during the mid-season, thus indicating that infiltrated and stored soil water played a major role in actual crop evapotranspiration.

The $ET_{c\,act}$ partition reported in Table 6 shows that soil evaporation, E_s, was the dominant component of the evapotranspiration process during the non-growing and initial stages. E_s values ranged from 63% to 72% of $ET_{c\,act}$ because rainfall is then larger and more frequent, thus keeping the soil wet most of the time. On the contrary, E_s were much smaller during the mid-season (from 16% to 24%) because a few precipitation events occurred, and drip irrigation was applied mostly under the canopies and at nighttime. It was found that E_s values during the entire crop season represented 39% to 40% of $ET_{c\,act}$, with the latter value referring to the wettest year, when the number of precipitation events was higher. Naturally, transpiration represented the largest fraction of the total $ET_{c\,act}$, which indicates that water use was quite efficient.

Table 6. Olives' actual evapotranspiration ($ET_{c\,act}$) and its partitioning into soil evaporation (E_s) and actual transpiration ($T_{c\,act}$), and ratios between soil evaporation and actual evapotranspiration ($E_s/ET_{c\,act}$, %) between actual crop transpiration and actual evapotranspiration ($T_{c\,act}/ET_{c\,act}$, %) and between actual evapotranspiration and potential evapotranspiration ($ET_{c\,act}/ET_c$, %) throughout the diverse crop stages and years.

	Year	Non-Growing	Initial	Development	Mid-Season	Late-Season	Whole Year
$ET_{c\,act}$ (mm)	2009	132	34	108	366	87	726
	2010	138	41	96	301	83	656
	2011	155	39	101	386	106	787
E_s (mm)	2009	87	22	56	65	53	283
	2010	93	26	29	72	47	264
	2011	109	28	47	61	61	305
$T_{c\,act}$ (mm)	2009	45	12	52	301	34	443
	2010	45	15	67	229	36	392
	2011	46	11	54	325	45	482
$E_s/ET_{c\,act}$ (%)	2009	66	65	52	18	61	39
	2010	67	63	30	24	57	40
	2011	70	72	47	16	58	39
$T_{c\,act}/ET_{c\,act}$ (%)	2009	34	35	48	82	39	61
	2010	33	37	70	76	43	60
	2011	30	28	53	84	42	61
$ET_{c\,act}/ET_c$ (%)	2009	100	100	100	96	100	98
	2010	100	100	100	84	98	91
	2011	100	100	100	99	100	99

3.4. Assessing the Applicability of the A&P Approach

The parameterization of the A&P approach was performed using the available average values of f_c observed for the mid- and end seasons (0.35) and the average h = 3.5 m. The selected value for the parameter M_L was 1.5, as proposed by Pereira et al. [33] for a traditional olive orchard with medium tree density. As discussed in that study, due to some uncertainty in the targeted K_{cb} values, two values for $F_{r\,mid}$ and $F_{r\,end}$ were used, one relative to a K_{cb} central value ($K_{cb\,A\&P\,central}$) and the other to an upper value ($K_{cb\,A\&P\,upper}$). Thus, $F_{r\,mid\,central}$ = 0.60, $F_{r\,end\,central}$ = 0.52, $F_{r\,mid\,upper}$ = 0.68, and $F_{r\,end\,upper}$ = 0.60 were used with Equation (14). These F_r values show the ability of olive trees to perform differentiated stomatal control throughout the season, with slightly higher stomatal control at the end season when compared with the mid-season. Applying Equations (12)–(14), the following $K_{cb\,A\&P}$ values were computed: $K_{cb\,A\&P\,mid\,central}$ = 0.40 and $K_{cb\,A\&P\,end\,central}$ = 0.35, and for the upper values $K_{cb\,A\&P\,mid\,upper}$ = 0.45 and $K_{cb\,A\&P\,end\,upper}$ = 0.40. In the following, these $K_{cb\,A\&P}$ values were used to compute $T_{c\,act\,A\&P}$ and these estimations were compared with $T_{SF\,field}$. The goodness-of-fit indicators relative to this comparison are presented in Table 7.

Table 7. Goodness-of-fit indicators relative to the comparison between transpiration obtained from sap-flow measurements ($T_{SF\,field}$) with the transpiration estimated with the A&P approach ($T_{c\,act\,A\&P}$).

		n	b_0	R^2	PBIAS (%)	RMSE (mm d^{-1})	AAE (mm d^{-1})	EF
A&P, 2009	Central value	104	1.01	0.68	2.5	0.28	0.21	0.67
	Upper value		1.13	0.68	15.3	0.43	0.35	0.26
A&P, 2011	Central value	145	0.91	0.81	−8.1	0.31	0.25	0.71
	Upper value		1.02	0.81	3.3	0.27	0.21	0.78

Central—corresponds to the central value of $K_{cb\,A\&P}$ for the mid- and end-season stages, of 0.40 and 0.35, respectively; Upper—corresponds to the upper limit value of $K_{cb\,A\&P}$, 0.45 and 0.40, respectively.

The results show that using the $K_{cb\ A\&P}$ central values, the RMSE values are nearly similar to those obtained when using the SIMDualKc model (Table 4). However, the A&P approach led to a lower performance due to the insufficient number of f_c and h observations, since it was intended to adjust $K_{cb\ A\&P}$ along the season. The RMSE values were higher for the drier season of 2009 and when the $K_{cb\ A\&P}$ upper values were used. These differences were expectable because by 2009 there was higher water stress during the mid-season stage (as depicted in Figure 3), which was not perceived when using the A&P approach due to the lack of adequate f_c surveillance which would allow the adjustment of the $K_{c\ A\&P\ upper}$ value.

Table 8 shows the estimated time-averaged $K_{cb\ act}$ values for the mid- and end-season stages obtained using the A&P approach, as well as the SIMDualKc model for the experimental years 2009 and 2011.

Table 8. Estimated time-averaged $K_{cb\ act}$ values for the mid- and end-season stages using the A&P approach and the SIMDualKc model for the experimental years 2009 and 2011.

	Approach	Growth Stage	
		Mid-Season	End-Season
2009	A&P central value	0.40	0.30
	A&P upper value	0.45	0.35
	SIMDualKc	0.39	0.37
2011	A&P central value	0.40	0.30
	A&P upper value	0.45	0.35
	SIMDualKc	0.41	0.37

Overall, results show that during the mid-season the $K_{cb\ A\&P}$ central value and during the end-season the $K_{cb\ A\&P}$ upper value are adequate for the prevailing conditions of the studied olive grove, which is in line with the K_{cb} values derived when calibrating the SIMDualKc model.

4. Conclusions

The SIMDualKc model was successfully calibrated and validated for an irrigated olive orchard in Sicily using transpiration data acquired with sap-flow sensors. Estimation errors associated with actual crop transpiration were fairly small, with an average RMSE of 0.26 mm d^{-1}. The performance of the model confirmed the appropriateness of the SIMDualKc model for estimating the $T_{c\ act}$ of olive orchards and supports the quality of the water balance results obtained.

The calibration and validation of SIMDualKc allowed us to derive updated single and basal crop coefficient curves for the investigated olive orchard. Since olives are perennials, in addition to the common crop stages proposed by FAO56, K_c and K_{cb} values were considered for the non-growing period. Greatly contrasting K_c and K_{cb} curves were obtained, analogous to those previously obtained for a super-intensive olive orchard. Although K_{cb} values do not include the effects of soil evaporation, the latter may be the largest fraction in K_c. Thus, while K_{cb} is larger when $T_{c\ act}$ is high during the mid-season, K_c is larger when the sum of $K_{cb} + K_e$ is greater, which happens when E_s is large. In contrast, K_c is smaller under limited rainfall and soil evaporation conditions. Contrastingly, K_{cb} is smaller when actual crop transpiration is limited by the available soil water and/or solar radiation. This means that K_{cb} is larger during the mid-season, when K_c is smaller and, on the contrary, K_{cb} is smaller during the non-growing period when K_c is high. These results were only evident when the study focused on the full year and not only on the growing season.

Using the SIMDualKc model, it was possible to define the standard K_{cb} values for the initial, mid-season, end-season, and non-growing periods, which were 0.30, 0.42, 0.37, and 0.30 respectively. On the other hand, the dependency of K_c on soil evaporation and

on rainfall events makes it difficult to define a standard K_c value for periods exhibiting a large inter-annual variability of rainfall. Therefore, the results for the initial, end, and non-growing seasons showed a large inter-annual variability in K_c values: $K_{c\,mid} = 0.55$ (average between 0.54 and 0.56), $K_{c\,ini} = 0.92$, and $K_{c\,end} = 0.95$ and $K_{c\,non\text{-}growing} = 0.93$. This behavior is common to other woody perennial crops. The use of the dual crop coefficient approach is likely to be more appropriate when assessing crop water use during the crop season and when precision irrigation is desired, whereas the single crop coefficient is likely to be more appropriate when performing less accurate soil water balance measurements for irrigation. The use of the dual K_c approach makes it easier to assess both soil evaporation and crop transpiration, thus providing a better understanding of the dynamics of $ET_{c\,act}$ under conditions of incomplete ground cover, as for orchards.

Results of the partitioning of $ET_{c\,act}$ with SIMDualKc show that the $E_s/ET_{c\,act}$ ratio was higher during the non-growing and initial periods when E_s was mainly influenced by the frequent rainfall events. Contrarily, that ratio was smaller during the mid-season, when the transpiration ratio $T_{c\,act}/ET_{c\,act}$ was greater.

The results confirm the suitability of the SIMDualKc model to simulate the terms of the soil water balance of the olive orchards and to derive the respective single and basal crop coefficients for irrigation scheduling purposes. Nevertheless, further studies are required to improve the model outputs, aimed at providing advice to farmers, specifically for designing appropriate irrigation scheduling strategies to save water and enhance yields and oil quality, as well as combining higher water productivity with reducing the water footprint of olives.

The assessment of the usability of the A&P approach with the observed f_c and h values, along with the calibrated/tabulated M_L and F_r values, showed appropriate results for the estimation of $T_{c\,act}$ when the central $K_{cb\,A\&P}$ is targeted. The results were constrained by the lack of measured f_c and h values required to identify the crop coefficient during the entire crop season. Further applications may support the extensive use of the A&P approach, which may aid in parameterizing soil water balance models that are used to support the enhancement of yields, water productivity, and to provide water savings.

List of Symbols and Abbreviations

A	Area (m^2)
AAE	Average Absolute Error (units of the variable)
A&P	Allen and Pereira approach (see [31])
a_D	Parameter of the deep percolation equation related with the available soil water at saturation and field capacity (mm)
b_D	Parameter of the deep percolation equation related with drainage characteristics of the soil (mm)
b_0	Regression coefficient of the linear regression forced to the origin (-)
CN	Curve Number (dimensionless)
CR	Capillary Rise (mm)
D_r	Depth of cumulative evapotranspiration (depletion) from the root zone (mm)
DP	Deep Percolation (mm)
E_s	Evaporation from the soil ($mm\ d^{-1}$ or $mm\ h^{-1}$)
EF	Efficiency of modelling (dimensionless)
ET_c	Crop evapotranspiration under standard conditions ($mm\ d^{-1}$ or $mm\ h^{-1}$)
$ET_{c\ act}$	Actual crop evapotranspiration, i.e., under non-standard conditions ($mm\ d^{-1}$ or $mm\ h^{-1}$)
ET_o	(Grass) Reference crop evapotranspiration ($mm\ d^{-1}$ or $mm\ h^{-1}$)
f_c	Fraction of soil surface covered by vegetation (dimensionless)
f_{ew}	Fraction of soil that is both exposed and wetted (dimensionless)
f_w	Fraction of soil surface wetted by rain or irrigation (dimensionless)
F	Sap flux ($m^3\ s^{-1}$)
F_r	Resistance correction factor (dimensionless)
h	Crop height (m)
I	Irrigation depth (mm)
K_c	(Standard) crop coefficient (dimensionless)
$K_{c\ act}$	Actual crop coefficient (under non-standard conditions) (dimensionless)
$K_{c\ ini}$	Crop coefficient during the initial growth stage (dimensionless)
$K_{c\ mid}$	Crop coefficient during the mid-season growth stage (dimensionless)
$K_{c\ end}$	Crop coefficient at end of the late-season growth stage (dimensionless)
$K_{c\ max}$	Maximum value of crop coefficient (dimensionless)
$K_{c\ min}$	Minimum value of crop coefficient (dimensionless)
$K_{c\ non\text{-}growing}$	Crop coefficient during the non-growing crop stage (dimensionless)
K_{cb}	Basal crop coefficient (dimensionless)
$K_{cb\ cover}$	Basal crop coefficient of the ground cover in the absence of tree foliage (dimensionless)
$K_{cb\ full}$	Basal crop coefficient during mid-season (at peak plant size or height) for vegetation with full ground cover or LAI > 3 (dimensionless)
$K_{cb\ ini}$	Basal crop coefficient during the initial growth stage (dimensionless)
$K_{cb\ mid}$	Basal crop coefficient during the mid-season growth stage (dimensionless)
$K_{cb\ end}$	Basal crop coefficient at end of the late-season growth stage (dimensionless)
$K_{cb\ non\text{-}growing}$	Basal crop coefficient during the non-growing crop stage (dimensionless)
K_d	Crop density coefficient (dimensionless)
K_e	Soil evaporation coefficient (dimensionless)
$K_{e\ max}$	Maximum value of K_e coefficient (following rain or irrigation) (dimensionless)
K_r	Soil evaporation reduction coefficient (dimensionless)
K_s	Water stress coefficient (dimensionless)
LAI	Leaf area index (m^2 (leaf area) m^{-2} (soil surface))
LAI_{field}	Field leaf area index ($m^2\ m^{-2}$)

LAI_{plant}	Plant leaf area index ($m^2 \, m^{-2}$)
M_L	Multiplier on f_c describing the effect of canopy density (dimensionless)
MSE	Mean square error (units of the variable)
P	Precipitation (mm)
PBIAS	Percent bias (%)
p	Soil water depletion fraction for no stress (dimensionless)
R^2	Coefficient of determination (dimensionless)
RAW	Readily available soil water of the root zone (mm)
REW	Readily evaporable water from the soil surface layer (mm)
RH_{min}	Daily minimum relative humidity (%)
RMSE	Root mean square error (units of the variable)
RO	Surface runoff (mm)
r_l	(Bulk) mean stomatal resistance of well-illuminated leaf ($s \, m^{-1}$)
r_{typ}	(Bulk) typical stomatal resistance of well-illuminated leaf ($s \, m^{-1}$)
T_c	Crop transpiration ($mm \, d^{-1}$ or $mm \, h^{-1}$)
$T_{c \, act}$	Actual crop transpiration ($mm \, d^{-1}$ or $mm \, h^{-1}$)
T_{max}	Daily maximum air temperature (°C)
T_{min}	Daily minimum air temperature (°C)
$T_{SF \, field}$	Field daily transpiration ($mm \, d^{-1}$)
$T_{SF \, plant}$	Plant daily transpiration depth ($mm \, d^{-1}$)
TAW	Total available soil water in the root zone (mm)
TEW	Total evaporable water from the soil surface layer (mm)
t	Time (h or d)
u_2	Wind speed observed, or adjusted to 2 m above ground surface ($m \, s^{-1}$)
Z_e	Depth of the surface soil layer subjected to drying by evaporation (m)
γ	Psychrometric constant ($kPa \, °C^{-1}$)
ΔT	Difference of temperature (°C)
ΔT_{max}	Maximum difference of temperatures (°C)
θ_{FC}	Soil water content at field capacity ($m^3 \, m^{-3}$)
θ_{WP}	Soil water content at the permanent wilting point ($m^3 \, m^{-3}$)
ν	Sap flow density ($m^3 \, m^{-2} \, s^{-1}$)

References

1. Duarte, F.; Jones, N.; Fleskens, L. Traditional olive orchards on sloping land: Sustainability or abandonment? *Environ. Manag.* **2007**, *89*, 86–98. [CrossRef] [PubMed]
2. Tanasijevic, L.; Todorovic, M.; Pizzigalli, C.; Lionello, P.; Pereira, L.S. Impacts of climate change on olives crop evapotranspiration and irrigation water requirements in the Mediterranean Region. *Agric. Water Manag.* **2014**, *144*, 54–68. [CrossRef]
3. Freixa, E.; Gil, J.M.; Tous, J.; Hermoso, J.F. Comparative study of the economic viability of high- and super-high-density olive orchards in Spain. *Acta Hortic.* **2011**, *924*, 247–254. [CrossRef]
4. Paço, T.A.; Pôças, I.; Cunha, M.; Silvestre, J.C.; Santos, F.L.; Paredes, P.; Pereira, L.S. Evapotranspiration and crop coefficients for a super intensive olive orchard. An application of SIMDualKc and METRIC models using ground and satellite observations. *J. Hydrol.* **2014**, *519*, 2067–2080. [CrossRef]
5. Paço, T.A.; Paredes, P.; Pereira, L.S.; Silvestre, J.; Santos, F.L. Crop coefficients and transpiration of a super intensive Arbequina olive orchard using the dual Kc approach and the K_{cb} computation with the fraction of ground cover and height. *Water* **2019**, *11*, 383. [CrossRef]
6. De Gennaro, B.; Notarnicola, B.; Roselli, L.; Tassielli, G. Innovative olive-growing models: An environmental and economic assessment. *J. Clean. Prod.* **2011**, *28*, 70–80. [CrossRef]
7. Paço, T.A.; Ferreira, M.I.; Rosa, R.D.; Paredes, P.; Rodrigues, G.C.; Conceição, N.; Pacheco, C.A.; Pereira, L.S. The dual crop coefficient approach using a density factor to simulate the evapotranspiration of a peach orchard: SIMDualKc model versus eddy covariance measurements. *Irrig. Sci.* **2012**, *30*, 115–126. [CrossRef]
8. Russo, C.; Cappelletti, G.M.; Nicoletti, G.M.; Di Noia, A.E.; Michalopoulos, G. Comparison of European olive production systems. *Sustainability* **2016**, *8*, 825. [CrossRef]
9. Iniesta, F.; Testi, L.; Orgaz, F.; Villalobos, F.J. The effects of regulated and continuous deficit irrigation on the water use, growth and yield of olive trees. *Eur. J Agron.* **2009**, *30*, 258–265. [CrossRef]
10. Trentacoste, E.R.; Puertas, C.M.; Sadras, V.O. Effect of irrigation and tree density on vegetative growth, oil yield and water use efficiency in young olive orchard under arid conditions in Mendoza, Argentina. *Irrig. Sci.* **2015**, *33*, 429–440. [CrossRef]
11. Pereira, L.S. Water, agriculture and food: Challenges and issues. *Water Resour. Manag.* **2017**, *31*, 2985–2999. [CrossRef]
12. Allen, R.G.; Pereira, L.S.; Raes, D.; Smith, M. Crop Evapotranspiration, Guidelines for Computing Crop Water Requirements. In *FAO Irrigation and Drainage Paper No. 56*; FAO: Rome, Italy, 1998; 300p.

13. Pereira, L.S.; Allen, R.G.; Smith, M.; Raes, D. Crop evapotranspiration estimation with FAO56: Past and future. *Agric. Water Manag.* **2015**, *147*, 4–20. [CrossRef]
14. Rallo, G.; Paço, T.A.; Paredes, P.; Puig-Sirera, À.; Massai, R.; Provenzano, G.; Pereira, L.S. Updated single and dual crop coefficients for tree and vine fruit crops. *Agric. Water Manag.* **2021**, *250*, 106645. [CrossRef]
15. Testi, L.; Villalobos, F.J.; Orgaz, F. Evapotranspiration of a young irrigated olive orchard in southern Spain. *Agric. For. Meteorol.* **2004**, *121*, 1–18. [CrossRef]
16. Allen, R.G.; Pereira, L.S.; Smith, M.; Raes, D.; Wright, J.L. FAO-56 dual crop coefficient method for estimating evaporation from soil and application extensions. *J. Irrig. Drain. Eng.* **2005**, *131*, 2–13. [CrossRef]
17. Er-Raki, S.; Chehbouni, A.; Boulet, G.; Williams, D.G. Using the dual approach of FAO-56 for partitioning ET into soil and plant components for olive orchards in a semi-arid region. *Agric. Water Manag.* **2010**, *97*, 1769–1778. [CrossRef]
18. Rallo, G.; Baiamonte, G.; Juárez, J.M.; Provenzano, G. Improvement of FAO-56 model to estimate transpiration fluxes of drought tolerant crops under soil water deficit: Application for olive groves. *J. Irrig. Drain. Eng.* **2014**, *140*, A4014001. [CrossRef]
19. Cammalleri, C.; Anderson, M.C.; Ciraolo, G.; D'Urso, G.; Kustas, W.P.; La Loggia, G.; Minacapilli, M. Applications of a remote sensing-based two-source energy balance algorithm for mapping surface fluxes without in situ air temperature observations. *Remote Sens. Environ.* **2012**, *124*, 502–515. [CrossRef]
20. Conceição, N.; Tezza, L.; Häusler, M.; Lourenço, S.; Pacheco, C.; Ferreira, I. Three years of monitoring evapotranspiration components and crop and stress coefficients in a deficit irrigated intensive olive orchard. *Agric. Water Manag.* **2017**, *191*, 138–152. [CrossRef]
21. Pereira, L.S.; Paredes, P.; Jovanovic, N. Soil water balance models for determining crop water and irrigation requirements and irrigation scheduling focusing on the FAO56 method and the dual Kc approach. *Agric. Water Manag.* **2020**, *241*, 106357. [CrossRef]
22. Santos, C.; Lorite, I.J.; Allen, R.G.; Tasumi, M. Aerodynamic parameterization of the satellite-based energy balance (METRIC) model for ET estimation in rainfed olive orchards of Andalusia, Spain. *Water Resour. Manag.* **2012**, *26*, 3267–3283. [CrossRef]
23. Cammalleri, C.; Rallo, G.; Agnese, C.; Ciraolo, G.; Minacapilli, M.; Provenzano, G. Combined use of eddy covariance and sap flow techniques for partition of ET fluxes and water stress assessment in an irrigated olive orchard. *Agric. Water Manag.* **2013**, *120*, 89–97. [CrossRef]
24. Pôças, I.; Paço, T.A.; Cunha, M.; Andrade, J.A.; Silvestre, J.; Sousa, A.; Santos, F.L.; Pereira, L.S.; Allen, R.G. Satellite based evapotranspiration of a super-intensive olive orchard: Application of METRIC algorithm. *Biosyst. Eng.* **2014**, *128*, 69–81. [CrossRef]
25. Pôças, I.; Paço, T.A.; Paredes, P.; Cunha, M.; Pereira, L.S. Estimation of actual crop coefficients using remotely sensed vegetation indices and soil water balance modelled data. *Remote Sens.* **2015**, *7*, 2373–2400. [CrossRef]
26. Autovino, D.; Rallo, G.; Provenzano, G. Predicting soil and plant water status dynamic in olive orchards under different irrigation systems with Hydrus-2D: Model performance and scenario analysis. *Agric. Water Manag.* **2018**, *203*, 225–235. [CrossRef]
27. Rosa, R.D.; Paredes, P.; Rodrigues, G.C.; Alves, I.; Fernando, R.M.; Pereira, L.S.; Allen, R.G. Implementing the dual crop coefficient approach in interactive software. 1. Background and computational strategy. *Agric. Water Manag.* **2012**, *103*, 8–24. [CrossRef]
28. Rosa, R.D.; Paredes, P.; Rodrigues, G.C.; Fernando, R.M.; Alves, I.; Pereira, L.S.; Allen, R.G. Implementing the dual crop coefficient approach in interactive software: 2. Model testing. *Agric. Water Manag.* **2012**, *103*, 62–77. [CrossRef]
29. Fandiño, M.; Cancela, J.J.; Rey, B.J.; Martínez, E.M.; Rosa, R.G.; Pereira, L.S. Using the dual-Kc approach to model evapotranspiration of Albariño vineyards (*Vitis vinifera* L. cv. Albariño) with consideration of active ground cover. *Agric. Water Manag.* **2012**, *112*, 75–87. [CrossRef]
30. Cancela, J.J.; Fandiño, M.; Rey, B.J.; Martínez, E.M. Automatic irrigation system based on dual crop coefficient, soil and plant water status for *Vitis vinifera* (cv Godello and cv Mencía). *Agric. Water Manag.* **2015**, *151*, 52–63. [CrossRef]
31. Allen, R.G.; Pereira, L.S. Estimating crop coefficients from fraction of ground cover and height. *Irrig. Sci.* **2009**, *28*, 17–34. [CrossRef]
32. Pereira, L.S.; Paredes, P.; Melton, F.; Johnson, L.; Wang, T.; López-Urrea, R.; Cancela, J.J.; Allen, R. Prediction of crop coefficients from fraction of ground cover and height. Background and validation using ground and remote sensing data. *Agric. Water Manag.* **2020**, *241*, 106197. [CrossRef]
33. Pereira, L.S.; Paredes, P.; Melton, F.; Johnson, L.; Mota, M.; Wang, T. Prediction of crop coefficients from fraction of ground cover and height. Practical application to vegetable, field and fruit crops with focus on parameterization. *Agric. Water Manag.* **2021**, *252*, 106663. [CrossRef]
34. Provenzano, G.; Rallo, G.; Ghazouani, H. Assessing field and laboratory calibration protocols for the diviner 2000 probe in a range of soils with different textures. *J. Irr. Drain. Eng.* **2016**, *142*, 04015040. [CrossRef]
35. Rallo, G.; Provenzano, G.; Castellini, M.; Puig-Sirera, À. Application of EMI and FDR sensors to assess the fraction of transpirable soil water over an olive grove. *Water* **2018**, *10*, 168. [CrossRef]
36. Rallo, L.; Torreño, P.; Vargas, A.; Alvarado, J. Dormancy and alternative bearing in olive. *Acta Hortic.* **1994**, *356*, 127–136. [CrossRef]
37. Sanz-Cortés, F.; Martinez-Calvo, J.; Badenes, M.L.; Bleiholder, H.; Hack, H.; LLácer, G.; Meier, U. Phenological growth stages of olive trees (*Olea europaea*). *Ann. Appl. Biol.* **2002**, *140*, 151–157. [CrossRef]
38. Orlandi, F.; Garcia-Mozo, H.; Vazquez Ezquerra, L.; Romano, B.; Dominguez, E.; Galan, C.; Fornaciari, M. Phenological olive chilling requirements in Umbria (Italy) and Andalusia (Spain). *Plant Biosyst.* **2004**, *138*, 111–116. [CrossRef]

39. Orlandi, F.; Sgromo, C.; Bonofiglio, T.; Ruga, L.; Romano, B.; Fornaciari, M. A comparison among olive flowering trends in different Mediterranean areas (south-central Italy) in relation to meteorological variations. *Theor. Appl. Climatol.* **2009**, *97*, 339–347. [CrossRef]

40. Rallo, G.; Provenzano, G. Modelling eco-physiological response of table olive trees (*Olea europaea* L.) to soil water deficit conditions. *Agric. Water Manag.* **2013**, *120*, 79–88. [CrossRef]

41. Granier, A. Evaluation of transpiration in a Douglas-fir stand by means of sap flow measurements. *Tree Physiol.* **1987**, *3*, 309–320. [CrossRef]

42. González-Altozano, P.; Pavel, E.W.; Oncins, J.A.; Doltra, J.; Cohen, M.; Gonza, P.; Paço, T.A.; Massai, R.; Castel, J.R. Comparative assessment of five methods of determining sap flow in peach trees. *Agric. Water Manag.* **2008**, *95*, 503–515. [CrossRef]

43. Siqueira, J.M.; Paço, T.A.; Silvestre, J.C.; Santos, F.L.; Falcão, A.O.; Pereira, L.S. Generating fuzzy rules by learning from olive tree transpiration measurement—An algorithm to automatize Granier sap flow data analysis. *Comput. Electron. Agric.* **2014**, *101*, 1–10. [CrossRef]

44. Valancogne, C.; Granier, A. Mesures de flux de sève brut. In *L'eau Dans L'espace Rural. Production Végétale et Qualité de L'eau*; Riou, C., Bonhomme, R., Chassin, P., Neveu, A., Papy, F., Eds.; INRA: Paris, France, 1997; pp. 153–160.

45. Motisi, A.; Rossi, F.; Consoli, S.; Papa, R.; Minacapilli, M.; Rallo, G.; Cammalleri, C.; D'Urso, G. Eddy covariance and sap flow measurements of energy and mass exchanges of woody crops in a Mediterranean environment. *Acta Hortic.* **2012**, *951*, 121–127. [CrossRef]

46. Villalobos, F.J.; Orgaz, F.; Mateos, L. Non-destructive measurement of leaf area in olive (*Olea europaea* L.) trees using a gap inversion method. *Agric. For. Meteorol.* **1995**, *73*, 29–42. [CrossRef]

47. Allen, R.G.; Wright, J.L.; Pruitt, W.O.; Pereira, L.S.; Jensen, M.E. Water requirements. In *Design and Operation of Farm Irrigation Systems*, 2nd ed.; Hoffman, G.J., Evans, R.G., Jensen, M.E., Martin, D.L., Elliot, R.L., Eds.; ASABE: St. Joseph, MI, USA, 2007; pp. 208–288.

48. Liu, Y.; Pereira, L.S.; Fernando, R.M. Fluxes through the bottom boundary of the root zone in silty soils: Parametric approaches to estimate groundwater contribution and percolation. *Agric. Water Manag.* **2006**, *84*, 27–40. [CrossRef]

49. Allen, R.G.; Pereira, L.S.; Howell, T.A.; Jensen, M.E. Evapotranspiration information reporting: I. Factors governing measurement accuracy. *Agric. Water Manag.* **2011**, *98*, 899–920. [CrossRef]

50. Pereira, L.S.; Paredes, P.; Rodrigues, G.C.; Neves, M. Modeling malt barley water use and evapotranspiration partitioning in two contrasting rainfall years. Assessing AquaCrop and SIMDualKc models. *Agric. Water Manag.* **2015**, *159*, 239–254, Corrigendum in **2016**, *163*, 408. [CrossRef]

51. Zhang, B.; Liu, Y.; Xu, D.; Zhao, N.; Lei, B.; Rosa, R.D.; Paredes, P.; Paço, T.A.; Pereira, L.S. The dual crop coefficient approach to estimate and partitioning evapotranspiration of the winter wheat—Summer maize crop sequence in North China Plain. *Irrig. Sci.* **2013**, *31*, 1303–1316. [CrossRef]

52. Moriasi, D.N.; Arnold, J.G.; Liew, M.W.; Van Bingner, R.L.; Harmel, R.D.; Veith, T.L. Model evaluation guidelines for systematic quantification of accuracy in watershed simulations. *Trans. ASABE* **2007**, *50*, 885–900. [CrossRef]

53. Wang, X.; Williams, J.; Gassman, P.W.; Baffaut, C.; Izaurralde, R.; Jeong, J.; Kiniry, J.R. EPIC and APEX: Model use, calibration, and validation. *Trans. ASABE* **2012**, *55*, 1447–1462. [CrossRef]

54. Nash, J.E.; Sutcliffe, J.V. River flow forecasting through conceptual models: Part 1. A discussion of principles. *J. Hydrol.* **1970**, *10*, 282–290. [CrossRef]

55. Villalobos, F.J.; Testi, L.; Orgaz, F.; García-Tejera, O.; Lopez-Bernal, A.; González-Dugo, M.V.; Ballester-Lurbe, C.; Castel, J.R.; Alarcón-Cabañero, J.J.; Nicolás-Nicolás, E.; et al. Modelling canopy conductance and transpiration of fruit trees in Mediterranean areas: A simplified approach. *Agric. For. Meteorol.* **2013**, *171–172*, 93–103. [CrossRef]

56. Martínez-Cob, A.; Faci, J.M. Evapotranspiration of an hedge-pruned olive orchard in a semiarid area of NE Spain. *Agric. Water Manag.* **2010**, *97*, 410–418. [CrossRef]

57. Villalobos, F.J.; Orgaz, F.; Testi, L.; Fereres, E. Measurement and modeling of evapotranspiration of olive (*Olea europaea* L.) orchards. *Eur. J. Agron.* **2000**, *13*, 155–163. [CrossRef]